Polymer Chemistry

ROYAL SOCIETY OF CHEMISTRY

PAPER

View Article Online
View Journal | View Issue

Cite this: *Polym. Chem.*, 2021, **12**, 6737

Molecular weight and dispersity affect chain conformation and pH-response in weak polyelectrolyte brushes†

Tzu-Han Li,[a] Megan L. Robertson *[b,c] and Jacinta C. Conrad *[b]

The impact of brush molecular weight distribution on the conformation and response of weak polyacid brushes was investigated. We show that weight-average degree of polymerization (N_w) and dispersity ($Đ$) alter the pH-responsive conformation of poly(acrylic acid) (PAA) brushes grafted to silica nanoparticles. We quantified the average brush length (l_b) at various pH using dynamic light scattering. The l_b of low-N_w PAA brushes (N_w = 45) increased as $Đ$ was increased from 1.09 to 1.69, but l_b for the high-N_w PAA brushes ($N_w \approx 813$) did not vary substantially when $Đ$ was increased from 1.23 to 1.76. This result indicates that the presence of a small fraction of long chains in a broad dispersity brush has a greater impact on l_b when N_w is low. Additionally, the extent of pH-response in $l_b/l_{b,max}$ increased with N_w or $Đ$ (when N_w is low), where the maximum brush length ($l_{b,max}$) was l_b measured at pH 10. The scaling of $l_b/l_{b,max}$ with degree of dissociation (α), however, was influenced by N_w but not $Đ$, indicating the low- and high-N_w PAA brushes were in the quasi-neutral brush (q-NB) and salted brush (SB) regimes, respectively. Differing behaviors in the pH-response and α-response of l_b at low N_w arose from subtle differences in dissociation behaviors among brushes of varying $Đ$. At low $Đ$, the low-N_w brush adopted a pH-independent extended conformation due to strong excluded volume interactions, whereas the conformation of the high-N_w brush varied from collapsed to stretched with increasing pH arising from electrostatic interactions. At high-$Đ$, we suggest the brush conformation also varied from collapsed to stretched with increasing pH regardless of N_w.

Received 7th August 2021,
Accepted 31st October 2021

DOI: 10.1039/d1py01056e

rsc.li/polymers

Introduction

Polyelectrolyte-grafted nanoparticles exhibit controllably reversible properties in response to pH change and are thus strong candidates for applications in colorimetric sensors,[1–3] filtration membranes,[4–7] and drug delivery.[8–11] The response of the brush conformation to environmental conditions, such as pH and added salt concentration C_s, is a key factor in the selection of materials for applications.[12,13] The extent of dissociation as pH is varied, however, depends on the polyelectrolyte, leading to different conformational responses to pH. Quenched polyelectrolyte brushes are highly extended by electrostatic interactions because the brushes are strongly dissociated and ionized at all pH values.[14,15] By contrast, for annealed brushes the degree of dissociation α varies with pH, leading to pH-responsive brush conformations induced by interchain and intrachain electrostatic interactions.[2,16–21] In addition to the effects of environmental conditions, the brush properties (*e.g.* molecular weight and grafting density σ) can also affect pH-response of chain conformation. Thus, there is great interest in understanding how to predict the conformation of polyelectrolyte brushes.

The conformation of spherical brushes has been described using a model for star polyelectrolytes accounting for a variety of interactions in the brush layer.[22] This model has been successfully applied to experimental studies on spherical polyelectrolyte brushes when $l_b/r_0 \geq 1$, where l_b is the average brush length and r_0 is the core radius.[23–26] The planar polyelectrolyte brush model, however, better predicts experimental results on

[a]*Materials Science and Engineering Program, University of Houston, Houston, Texas 77204, USA*
[b]*William A. Brookshire Department of Chemical Engineering, University of Houston, Houston, Texas, 77204, USA. E-mail: jcconrad@uh.edu, mlrobertson@uh.edu*
[c]*Department of Chemistry, University of Houston, Houston, Texas 77204, USA*

†Electronic supplementary information (ESI) available: Experimental details. TGA data of silica nanoparticles, initiator-grafted silica nanoparticles, P*t*BA brushes, and initiation efficiency. GPC refractometer chromatographs of cleaved P*t*BA. Proton NMR spectra of P*t*BA and PAA brushes. DLS intensity-intensity correlation curves of PAA brushes at pH 3, 7, and 10. $l_b/l_{b,max}$ of PAA brushes from this study and literature as a function of pH. pH titration data of PAA brushes including mole number of individual molecule and fitting titration curves. C_i of the PAA brushes at ionic strength 10^{-4} M. $l_b/l_{b,max}$ of the high-N_w PAA brushes and PDMAEMA brushes from literature as a function of α. Scaling of l_b of the PAA brushes with α. See DOI: 10.1039/d1py01056e

spherical polyelectrolyte brushes when $l_b/r_0 < 1$.[27–29] The star polyelectrolyte model, which predicts conformation of salt-added (quenched, or annealed when $\alpha = 1$) star polyelectrolytes as a function of the number of chains f and C_s, can be adapted to spherical polyelectrolyte brushes using $\sigma = f/4\pi r_0^2$ (Fig. 1).[22] In the Pincus regime (low σ), l_b is affected primarily by intra-chain and/or interchain electrostatic interactions.[22,30,31] In the osmotic brush (OsB) regime (intermediate σ), counterions from the bulk solution are strongly condensed in the brush layer and the osmotic pressure of counterions controls brush conformation.[16,22,23,31,32] In the quasi-neutral brush (q-NB) regime (high σ), polyelectrolyte brushes are more strongly affected by excluded volume interactions than electrostatic interactions.[22,31] In the salted brush (SB) regime, which occurs at high C_s, electrostatic interactions are screened by added salts.[22,23] In this regime, l_b increases with σ due to electrostatic excluded volume interactions, whereas it decreases with increasing C_s because of charge screening:[22]

$$l_b \sim aN^{3/5}\alpha^{2/5}(C_s a^3)^{-1/5}\sigma^{1/5} \quad (1)$$

where a is the monomer length and N is the number of repeat units. Identical scaling behaviour is observed for annealed spherical polyelectrolyte brushes in the presence of added salt regardless of α.[22,24–26] Nonetheless, the impact of brush properties, *e.g.* N, σ, and dispersity $Đ$, on the applicability of the star polyelectrolyte model in spherical polymer brush systems with high curvature has been underexplored.

A recent experimental study examined the extent of pH-response on conformation and the scaling of l_b of annealed polyelectrolyte poly(2-(dimethylamino)ethyl methacrylate) (PDMAEMA) grafted on spherical nanoparticles across a range of N, σ, and $Đ$ as a function of α at C_s of 1 mM.[26] This study found that l_b normalized by the maximum value for each brush collapsed onto a single curve as a function of pH, indicating that the extent of pH-response on brush conformation was independent of these properties.[26] Further, l_b of all brushes scaled as $\alpha^{0.26\pm0.02}$, suggesting that the electrostatic interactions among the brush layers were not sensitive to N, σ, and $Đ$.[26] By contrast, in another study, the extent of pH-response in the conformation of annealed polyelectrolyte poly(acrylic acid) PAA grafted on spherical nanoparticles varied with both weight-average degree of polymerization N_w and σ.[33] Therefore, it remains unclear how these brush properties affect the pH-response of the brush conformation and the driving forces for extension of the polymer chains.

Our prior study showed that $Đ$ differently affected conformation of neutral brushes at low and high N_w.[34] Here, we extend this work to investigate the conformation of polyelectrolyte brushes of varying N_w and $Đ$ as a function of pH. We synthesized low-N_w and high-N_w pairs of PAA brushes hydrolyzed from poly(*tert*-butyl acrylate) P*t*BA-grafted silica nanoparticles in which $Đ$ varied: in the first pair, $N_w = 45$ and $Đ = 1.09$ and 1.69; in the second pair, $N_w \approx 813$ and $Đ = 1.23$ and 1.76. The brush conformation was assessed by measuring l_b as a function of pH using dynamic light scattering. At $N_w = 45$, l_b of the high-$Đ$ brush was markedly greater than that of the corresponding low-$Đ$ brush for pH values ranging from 3 to 10, whereas at $N_w \approx 813$ the difference in l_b with $Đ$ was less pronounced. Increasing N_w or $Đ$ (when N_w is low) led to a greater extent of pH-response of $l_b/l_{b,max}$, where $l_{b,max}$ is l_b measured at pH 10. However, the scaling exponent of $l_b/l_{b,max}$ with α increased with increasing N_w but not $Đ$, suggesting the low-N_w and high-N_w brushes were in the q-NB and SB regimes, respectively (Fig. 1). Differences in pH- and α-responses of $l_b/l_{b,max}$ arose from subtle variations in the dissociation behaviour of the low-N_w brushes. Together, our results indicate that the low-N_w, low-$Đ$ brush adopted a pH-independent and extended conformation, whereas the conformation of brushes with higher N_w and/or $Đ$ varied from collapsed to extended with increasing pH as assessed from the brush properties (Table 1).

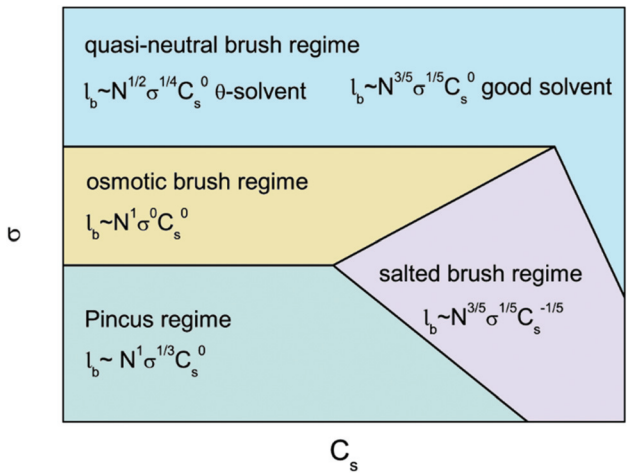

Fig. 1 State diagram for high curvature ($l_b/r_0 > 1$) spherical polymer brushes, derived from a model for salt-added quenched and annealed (when $\alpha = 1$) star polyelectrolytes with σ in a solution of C_s. Adapted from ref. 22.

Experimental

Materials

All chemicals were purchased from Sigma-Aldrich and used as received unless noted in the following. Dichloromethane (DCM, JT Baker, HPLC grade, ≥99.8%) was dried with a Pure Process Technology solvent purification system.

Table 1 Variables and their symbols in the present study

Variable	Symbols
Number-average degree of polymerization	N_n
Weight-average degree of polymerization	N_w
Dispersity	$Đ$
Grafting density	σ
Brush length	l_b
Degree of dissociation	α
Zeta potential	ζ

Synthetic procedures

The synthesis of P*t*BA-grafted nanoparticles, where r_0 = 5.7 ± 0.2 nm, has been previously reported,[34] and is summarized in the ESI.† Four P*t*BA-grafted nanoparticles were selected for hydrolysis to PAA-grafted nanoparticles (Table 2). The P*t*BA-grafted nanoparticles (110 mg) were transferred to a 100 mL round bottom flask and dissolved in 11 mL DCM under 375 rpm stirring at room temperature. 3 mL of trifluoroacetic acid was subsequently added to the solution for hydrolysis. The flasks were covered with aluminium foil and wrapped with Parafilm, and the reaction was allowed to proceed for 14 h at room temperature (Scheme 1). The solutions were dried under nitrogen purge and then dried in a vacuum oven at room temperature overnight. The remaining solid was dispersed in a minimum quantity of methanol (typically, 1 ml), precipitated into 100 mL DCM, and collected by centrifugation. The purification procedure was repeated three times and removal of unreacted monomer was confirmed by proton nuclear magnetic resonance (^{1}H-NMR). We note that the hydrolysis time is shorter than that used in earlier studies of planar PAA brushes, for which the hydrolysis did not appear to affect σ or $Đ$;[35,36] we therefore expect that $Đ$ and σ of polymer grafted on the nanoparticles is not affected by the hydrolysis protocol.

Table 2 P*t*BA-grafted silica nanoparticles selected for hydrolysis

P*t*BA brushes	N_w [a]	N_n [a]	$Đ$[a]	l_b [b] (nm)	σ[c] (chains per nm^2)
Low N_w, low $Đ$	45 ± 3	41 ± 4	1.09	6.6 ± 0.2	0.38
Low N_w, high $Đ$	45.3 ± 0.7	26 ± 3	1.69	14.0 ± 0.2	0.53
High N_w, low $Đ$	780 ± 50	630 ± 40	1.23	57.2 ± 0.3	0.31
High N_w, high $Đ$	840 ± 10	480 ± 30	1.76	58.0 ± 0.5	0.70

[a] Characterized with GPC: N_n and N_w were calculated using M_n/M_0 and M_w/M_0, respectively, where M_n is the number-average molecular weight, M_w is the weight-average molecular weight, and M_0 = 128 g mol^{-1} is the molecular weight of *t*BA; $Đ = N_w/N_n$. Standard deviations were calculated from 3 measurements. [b] Characterized with DLS: l_b was calculated using the method of cumulants (eqn (2) and (3)) to quantify the polymer-grafted nanoparticle R_h, followed by subtraction of r_0. Standard deviations were calculated from 10 measurements on the same sample. [c] Characterized with TGA and EA.[34]

Characterization procedures

Procedures for thermogravimetric analysis (TGA), elemental analysis (EA), gel permeation chromatography (GPC), and ^{1}H NMR have been previously reported[34] and are summarized in the ESI.†

Sample preparation

The PAA-grafted silica nanoparticles were dispersed at concentrations of 0.5 and 2 mg mL^{-1} for DLS/zeta potential and pH titration measurements, respectively, by stirring in Milli-Q water with varying pH for 3 h. pH was adjusted prior to dispersion by adding $HCl_{(aq)}$ and $NaOH_{(aq)}$ into Milli-Q water for acidic and basic conditions, respectively. The $HCl_{(aq)}$ and $NaOH_{(aq)}$ solutions were prepared using Milli-Q water to reduce the influence of unknown ionic strength from pre-existing ions. In addition, pH was measured thrice to confirm the stability of pH with 1 min stirring between individual pH readings. The samples were then filtered through a 0.2 or 0.45 μm Nylon syringe filter depending on the size of the nanoparticles.

Dynamic light scattering (DLS). l_b was determined *via* DLS. The intensity correlation function $g^{(2)}(q,t)$ was measured on a DLS setup consisting of an ALV goniometer, a He–Ne laser (wavelength λ = 632.8 nm), and an ALV-5000/EPP Multiple tau digital correlator (ALV-GmbH, Langen, Germany). Each measurement was performed for 60 s at a constant scattering angle θ = 90°. $g^{(2)}(q,t)$ was fit using the method of cumulants,[37]

$$g^{(2)}(q,t) - 1 = \left[Ae^{\left(\frac{-t}{\tau(q)}\right)\left(1+\frac{\mu t^2}{2}\right)} \right]^2 \quad (2)$$

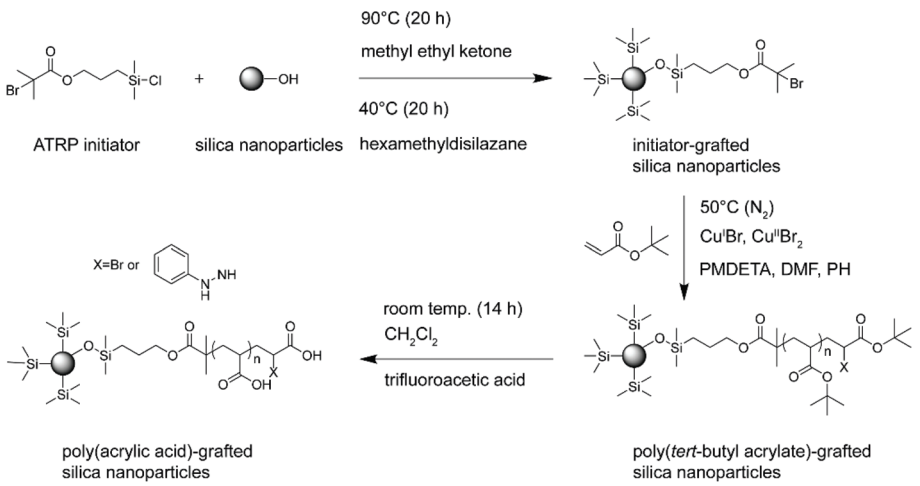

Scheme 1 Synthesis of PAA brushes.

where t is the lag time, which ranged from 2.5×10^{-4} to 10^{3} ms; q is the scattering vector ($q = 4\pi \sin(\theta/2)/\lambda$); τ^{-1} is the relaxation rate; and μ is the variance of the distribution. The hydrodynamic radius R_h was calculated from the diffusion coefficient D using the Stokes–Einstein equation

$$D = \frac{1}{\tau q^2} = \frac{k_B T}{6\pi\eta R_h} \quad (3)$$

where η is the viscosity of water at 20 °C, k_B is the Boltzmann constant, and T is the temperature.[38,39] The l_b was then obtained by subtracting r_0 from R_h. Three aqueous solutions were prepared from each brush on different days to determine the standard error on l_b. Measurements of l_b were repeated consecutively ten times for each solution.

Zeta potential (ζ). The ζ of PAA-grafted silica nanoparticles was measured using a NanoBrook ZetaPALS (Brookhaven Instruments) analyzer. Measurement of zeta potential was repeated 5 times on one solution for each brush to determine the standard deviation.

pH titration. pH values were measured by using a pH electrode InLab Micro Pro-ISM connected to a SevenCompact pH meter S220 (Mettler Toledo). To titrate the PAA brushes, the pH was adjusted to 12 by adding 0.5 M $NaOH_{(aq)}$ with a micropipette. The solution was then titrated with 0.5 M $HCl_{(aq)}$. The volume of the titrant was recorded from the micropipette, and the pH values were averaged from 3 measurements after each addition of the titrant.

Results and discussion

To understand the effect of chain $Đ$ on polyelectrolyte brush conformation, we measured l_b as a function of pH for two pairs of PAA brushes grafted on silica nanoparticles of similar N_w but different $Đ$. For the low-N_w series (N_w = 45), l_b of the low-$Đ$ PAA brush was independent of pH and was equal to the weight-average contour length $L_{c,w} = N_w l_0$, where l_0 = 0.3 nm is the monomer length (Fig. 2a). In sharp contrast, l_b of the high-$Đ$ PAA brush increased upon increasing pH and was markedly greater than both l_b of the low-$Đ$ PAA brush and $L_{c,w}$. The greater value of l_b of the high-$Đ$ PAA brush relative to that of the corresponding low-$Đ$ PAA brush and to $L_{c,w}$ can be attributed to the presence of long chains,[26] which increase the brush length measured in DLS beyond that expected for a uniform chain of a given N_w. For the high-N_w series ($N_w \approx 813$), l_b of both PAA brushes increased with pH and gradually approached their $L_{c,w}$. At high N_w, differences in l_b between the low and high-$Đ$ brushes were less pronounced than for the low-N_w brushes and were statistically insignificant at some pH values (Fig. 2b) Thus, $Đ$ differently affected l_b of brushes at low and high N_w. This result is consistent with the behaviour of neutral brushes observed in our previous study, in which l_b increased with $Đ$ at low N_w but was independent of $Đ$ for high N_w.[34] To examine the extent of pH-response, l_b was normalized by $l_{b,max}$. At low N_w, the high-$Đ$ brush exhibited a greater change in $l_b/l_{b,max}$ than the low-$Đ$ brush as a function of pH. At high N_w, however, $l_b/l_{b,max}$ of both low- and high-$Đ$ brushes collapsed with that of the low-N_w, high-$Đ$ brush (Fig. 2c). This comparison reveals that the extent of pH-response in l_b can be enhanced by increasing either N_w or $Đ$ (when N_w is low).

Prior studies report the pH-responsive $l_b/l_{b,max}$ in polybasic PDMAEMA brushes (N_w = 392–2541)[26] and polyacid PAA brushes (N_w = 250–1111).[33] $l_b/l_{b,max}$ of PDMAEMA or PAA brushes as a function of pH collapsed onto a single curve for brushes of differing N_w,[26] which is consistent with the behaviour we observed in the high-N_w PAA brushes (N_w = 782 and 837) (Fig. S8a†). We suggest the high-N_w PAA brushes were in a high-N_w regime where $l_b/l_{b,max}$ was dependent on pH. However, $l_b/l_{b,max}$ of the PAA brush with the lowest N_w probed in ref. 33 (N_w = 153) was independent of pH, consistent with the behaviour of our low-N_w, low-$Đ$ brush (N_w = 45) (Fig. S8b†). We suggest the low-N_w PAA brushes in our study were in a low-N_w regime, where $l_b/l_{b,max}$ was independent of pH and

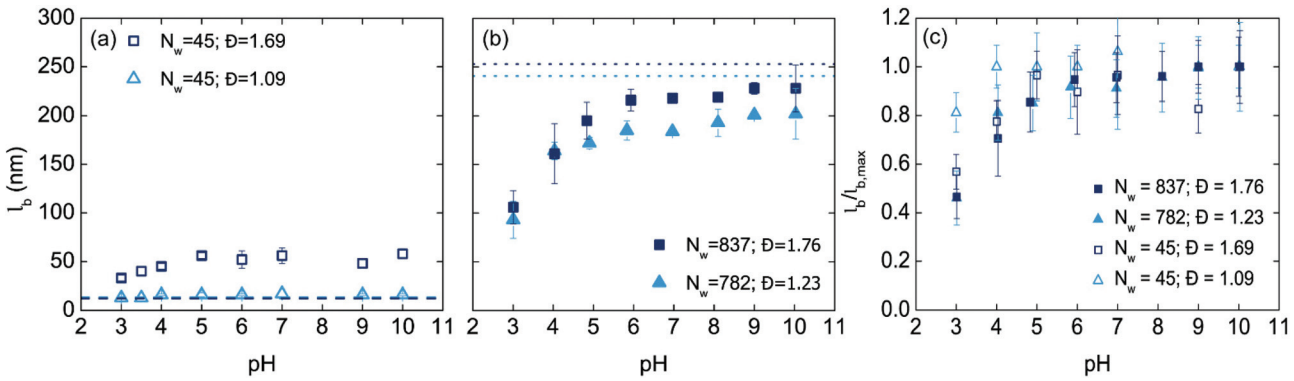

Fig. 2 l_b as a function of pH of the (a) low-N_w PAA brush pair with N_w = 45, $Đ$ = 1.09 (light blue open triangles) and N_w = 45, $Đ$ = 1.69 (dark blue open squares) and (b) high-N_w PAA brush pair with N_w = 782, $Đ$ = 1.23 (light blue closed triangles) and N_w = 837, $Đ$ = 1.76 (dark blue closed squares). (c) l_b was normalized by $l_{b,max}$ (l_b measured at pH 10) as a function of pH for four PAA brushes. Dashed and dotted lines in (a) and (b) indicate $L_{c,w}$ of the low-N_w and high-N_w PAA brush pairs, respectively. Light blue and dark blue lines represent $L_{c,w}$ of the low-$Đ$ and high-$Đ$ PAA brushes, respectively. Error of l_b, smaller than symbols if not visible, was determined from 3 independent DLS measurements.

increased with increasing $Đ$. To explain the differences in the extent of pH response among the PAA brushes, we posit that the dominant parameter controlling the brush conformation, α, exhibited distinct sensitivities to changes in $Đ$ in the two regimes of N_w investigated.

To test this idea, we determined α of the PAA brushes as a function of pH (Fig. 3) as assessed *via* titration curves upon decreasing pH (Fig. S9; procedures described in the ESI†).[40] α monotonically increased with pH, in agreement with the previously reported behaviour of annealed polyacid brushes.[41–44] The titration curves of the PAA brushes were qualitatively similar for brushes of different $Đ$ but similar N_w, indicating they were similarly dissociated and associated at high and low pH, respectively. To quantitatively examine the dissociation behaviour, the data were fit with sigmoidal curves, and the average acid dissociation constant pK_a was obtained as the pH at $\alpha = 0.5$ for each of the brushes.[45] At low N_w, pK_a = 6.14 ± 0.06 and 6.28 ± 0.06 for low-$Đ$ and high-$Đ$ brushes, respectively; at high N_w, pK_a = 5.68 ± 0.03 and 5.96 ± 0.01 for low-$Đ$ and high-$Đ$ brushes, respectively. These results indicate that the PAA brushes behave as annealed polyacids and bear an increasing number of negative charges as pH is increased. Further, increasing $Đ$ slightly increased pK_a whereas increasing N_w decreased pK_a. The weak dependence of pK_a on $Đ$ is consistent with an earlier study on planar PAA brushes, when pK_a was measured upon decreasing pH (as it was measured in the present study).[35] By contrast, pK_a of the planar PAA brushes drastically increased with $Đ$ when measured upon increasing pH.[35]

We characterized ζ as a function of pH (Fig. 4) to provide further insight into the dissociation behaviour of PAA brushes. The PAA brushes were negatively charged at all pH values tested and ζ monotonically decreased with increasing pH, indicating the number of charges increased for all brushes. The decrease in ζ with increasing N_w arises from greater number of dissociated repeat units.[46] These results suggest that the counterions (*i.e.* positive charges) in the bulk solution could condense in the brush layer due to electrostatic inter-

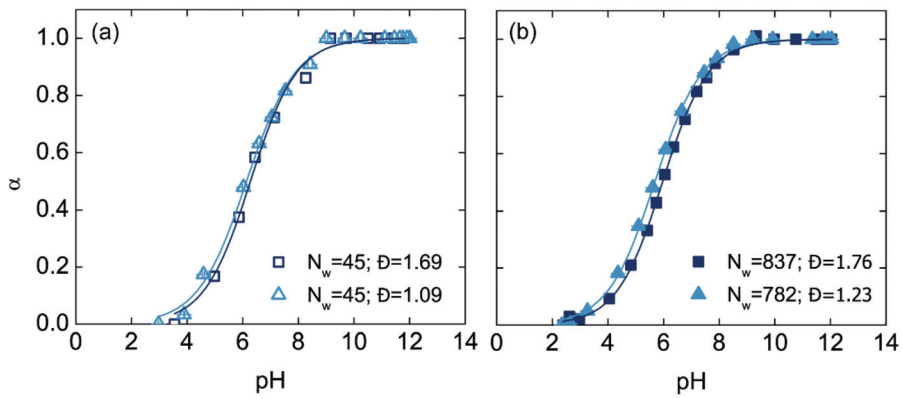

Fig. 3 α as a function of pH of the (a) low-N_w PAA brush pair with N_w = 45, $Đ$ = 1.09 (light blue open triangles) and N_w = 45, $Đ$ = 1.69 (dark blue open squares) and (b) high-N_w PAA brush pair with N_w = 782, $Đ$ = 1.23 (light blue closed triangles) and N_w = 837, $Đ$ = 1.76 (dark blue closed squares). Light and dark blue solid lines are sigmoidal fits shown in the ESI (eqn (S9)†) of the low-$Đ$ and the high-$Đ$ PAA brushes, respectively, and the results of fitting parameters are shown in Table S2 in the ESI.†

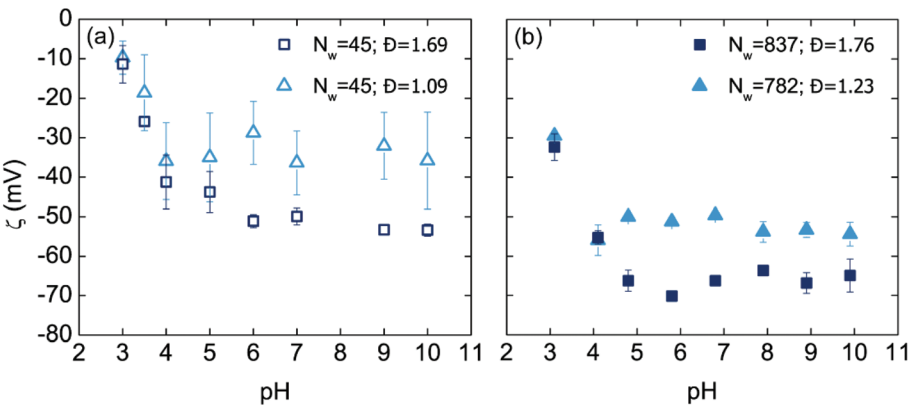

Fig. 4 ζ as a function of pH of the (a) low-N_w PAA brush pair with N_w = 45, $Đ$ = 1.09 (light blue open triangles) and N_w = 45, $Đ$ = 1.69 (dark blue open squares) and (b) high-N_w PAA brush pair with N_w = 782, $Đ$ = 1.23 (light blue closed triangles) and N_w = 837, $Đ$ = 1.76 (dark blue closed squares). Error of ζ, smaller than symbols if not visible, was determined from 5 repeated measurements.

actions with negative charges on polyelectrolyte chains, but could not completely neutralize the negative charges.[16,47] In addition, we calculated the concentration of condensed counterions C_i at pH 10 (α = 1); C_i was the largest for the low N_w, low $Đ$ brush (due to differences in l_b) (Fig. S11, equations are shown in the ESI†).

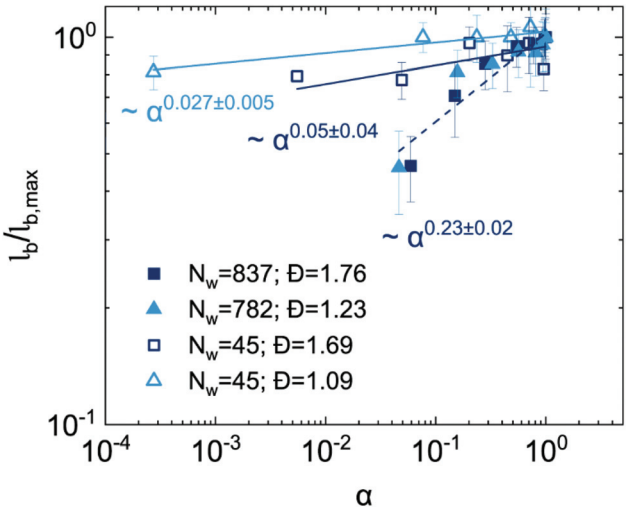

Fig. 5 $l_b/l_{b,max}$ as a function of α of the low-N_w PAA brush pair with N_w = 45, $Đ$ = 1.09 (light blue open triangles) and N_w = 45, $Đ$ = 1.69 (dark blue open squares) and the high-N_w PAA brush pair with N_w = 782, $Đ$ = 1.23 (light blue closed triangles) and N_w = 837, $Đ$ = 1.76 (dark blue closed squares). Data were fit to a power-law equation $\log l_b/l_{b,max} = b + c \times \log \alpha$, where b and c were intercept and slope, respectively. Solid lines indicate the fits for low-N_w brushes and the dashed line indicates the fit for the high-N_w brushes, which collapsed onto a single curve and were fit together. Fig. S13 in the ESI† shows l_b as a function of α.

To probe PAA brush swelling, $l_b/l_{b,max}$ was examined as a function of α, using the pH-dependencies of both $l_b/l_{b,max}$ (in Fig. 2c) and α (in Fig. 3, along with sigmoidal fits to the data).

$l_b/l_{b,max}$ of the low-N_w PAA brushes scaled weakly with α: $l_b/l_{b,max} \sim \alpha^{0.027\pm0.005}$ for the low-$Đ$ brush and $l_b/l_{b,max} \sim \alpha^{0.05\pm0.04}$ for the high-$Đ$ brush (Fig. 5). Although $Đ$ did not affect the scaling exponent for low-N_w brushes, brushes with lower $Đ$ had a greater degree of chain extension (*e.g.*, greater $l_b/l_{b,max}$) at a given value of α (Fig. 5). These scaling exponents indicate that the PAA brushes with N_w = 45 were in the q-NB regime and were more affected by short-range excluded volume interactions than long-range electrostatic interactions.[22,31] By contrast, $l_b/l_{b,max}$ for high-N_w brushes at both low- and high-$Đ$ collapsed onto a single curve with that of PDMAEMA brushes (Fig. S12†),[26] which had a larger scaling exponent: $l_b/l_{b,max} \sim \alpha^{0.23\pm0.02}$ (Fig. 5), consistent with the scaling of the SB regime from prior studies.[24,26] The transition from the q-NB to SB regimes upon increasing N_w is consistent with expectations from the star polyelectrolyte model.[22] Overall, $l_b/l_{b,max}$ collapsed as a function of α for the brushes with high but not low N_w (Fig. 5), and $l_b/l_{b,max}$ for the high-N_w brushes and the low-N_w, high-$Đ$ brush collapsed as a function of pH (Fig. 2c).

Increasing $Đ$ led to distinct behaviours for low-N_w brushes in the α- and pH-responses of $l_b/l_{b,max}$. Whereas the pH-dependence of $l_b/l_{b,max}$ showed a significant change as $Đ$ increased (Fig. 2c), the scaling of $l_b/l_{b,max}$ with α was unaffected by $Đ$ (Fig. 5). At high N_w, the pH- and α-responses of $l_b/l_{b,max}$ each

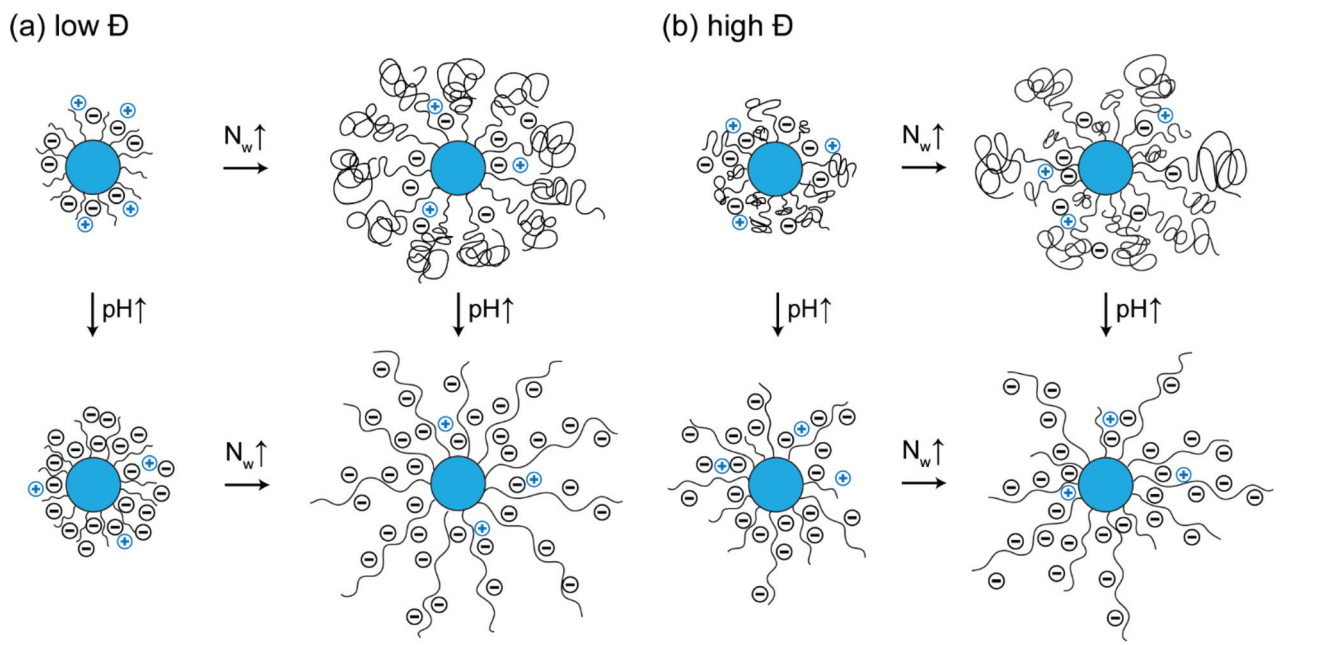

Fig. 6 Schematic representation of the conformation of annealed polyacid-grafted nanoparticles: (a) low $Đ$ and (b) high $Đ$ with variation of N_w and pH. The negative charges (black) are attributed to dissociated polyelectrolyte chains. The positive charges (blue) are attributed to counterions condensed from the bulk.

collapsed to a single curve as $Đ$ was varied (Fig. 2c and 5). These differences in relationships of $l_b/l_{b,max}$ with α and pH likely arise from subtle differences in dissociation behaviours among these brushes, quantified by the pK_a (Fig. 3). We can identify different regimes of behaviour in low- and high-N_w brushes using our data and that of a prior study. At high-N_w, the pH- and α-respsonses of $l_b/l_{b,max}$ each collapsed onto a single curve for PDMAEMA brushes (N_w = 392–2541; $Đ$ = 1.31–2.10).[26] This behaviour is consistent with our data on high-N_w PAA brushes (N_w = 782 and 837; $Đ$ = 1.23 and 1.76). Therefore, we suggest that these brushes were in the high-N_w regime, where the pH- and α-responses of $l_b/l_{b,max}$ each collapsed to a curve independent of N_w and $Đ$. By contrast, $l_b/l_{b,max}$ varied differently as a function of pH and α for the low-N_w PAA brushes in our study (N_w = 45; $Đ$ = 1.09 and 1.69). We hypothesize the low-N_w PAA brushes were in a low-N_w regime, where the relationships of pH- and α-responses of $l_b/l_{b,max}$ were affected by subtle differences in pK_a (low-$Đ$: pK_a = 6.14 ± 0.06 and high-$Đ$: 6.28 ± 0.06) (Fig. 3).

We propose schematic representations for low-$Đ$ (Fig. 6a) and high-$Đ$ (Fig. 6b) annealed polyacid-grafted nanoparticles. Because l_b of the low-N_w, low-$Đ$ PAA brush was approximately equal to $L_{c,w}$, we suggest that the brush adopted a near-fully extended conformation at low pH due to strong excluded volume interactions (the q-NB regime). Although increase in pH induced electrostatic interactions, the brush could not further extend (Fig. 6a).[33] The gradual increase of l_b to $L_{c,w}$ as pH increased for the high-N_w, low-$Đ$ PAA brush indicates that the conformation transitioned from a relatively collapsed state to a near-fully extended state with increasing pH (Fig. 6a). In the collapsed state, the brush was stretched near the particle surface arising from the proximity of neighbouring chains. Further from the surface, the greater inter-chain distance allowed the brush to adopt an entropically favourable coiled conformation. In the extended state, the chain extension was induced by electrostatic excluded volume interactions.[22]

The gradual increase of l_b to $L_{c,w}$ with increasing pH was also observed for the high-$Đ$ PAA brushes, in which the conformation varied from collapsed to stretched with increasing pH (Fig. 6b). In the collapsed state, the shorter chains of the high-$Đ$ brush adopted a "crown and stem" conformation at short distances from the surface, although the conformation at the periphery remained coiled.[48] We propose that the conformation of the high-$Đ$ brushes in the extended state was similar to that of the high-N_w, low-$Đ$ brush (Fig. 6b), evidenced by the collapse of $l_b/l_{b,max}$ on a single curve as a function of pH for these three brushes (Fig. 2c).

Conclusions

We investigated the dependence of l_b of annealed polyacid brushes and its pH-response on N_w and $Đ$. l_b increased with $Đ$ for the low- but not high-N_w PAA brushes. Increasing N_w or $Đ$ (in the case of low N_w brushes) enhanced the extent of pH-response of $l_b/l_{b,max}$, whereas the extent of α-response of $l_b/l_{b,max}$ increased with N_w but not $Đ$. The scaling exponents of $l_b/l_{b,max}$ with α indicated the brush regime changed from q-NB to SB upon increasing N_w. Differences in pH- and α-responses of $l_b/l_{b,max}$ at low N_w were attributed to differences in the dissociation behaviours, quantified by pK_a. We propose that the low-N_w, low-$Đ$ brush adopted a near-fully extended conformation at low pH arising from strong excluded volume interactions. Although increase in pH induced greater electrostatic interactions, the brush conformation did not change because the brushes were almost fully extended. By contrast, l_b of brushes with higher N_w and/or $Đ$ greatly increased with pH. We hypothesize that the brush conformation transitioned from collapsed to extended with increasing pH. The pH-dependence of conformation of annealed polyelectrolyte brushes can therefore be tuned by varying N_w or $Đ$ (when N_w is low). This understanding of the effects of brush properties on the extent of pH-responsiveness of the brush conformation can be leveraged for applications of annealed polyelectrolyte brushes. For example, short (<10 nm) brushes have been applied as adsorbents for water pollutants[43] and as colorimetric sensors;[1] we expect that modulating the length distribution of these brushes may lead to enhancements in efficacy. Indeed, we anticipate that different synthesis routes may lead to various distributions of brush molecular weight[49] and hence distinctive structure–property relationships.[50] Thus, we expect that tailoring the molecular weight distribution will provide additional control over the properties of responsive brushes.

Conflicts of interest

There are no conflicts to declare.

Acknowledgements

We thank Peter Vekilov and Ramanan Krishnamoorti for access to the dynamic light scattering and thermogravimetric analysis instruments, respectively. We thank Jeffrey Rimer for access to the HF fume hood and Ali Slim for assisting with HF experiments. We thank Scott Smith for access to the University of Houston Department of Chemistry Nuclear Magnetic Resonance Facility. Finally, we acknowledge the Welch Foundation (E-1869), American Chemical Society Petroleum Research Fund (58531-ND7), National Science Foundation (DMR-1611376), and the University of Houston Grants to Enhance and Advance Research Program.

Notes and references

1 K. Paek, S. Chung, C.-H. Cho and B. J. Kim, *Chem. Commun.*, 2011, **47**, 10272–10274.
2 K. Paek, H. Yang, J. Lee, J. Park and B. J. Kim, *ACS Nano*, 2014, **8**, 2848–2856.
3 Y. Ma, K. Promthaveepong and N. Li, *Anal. Chem.*, 2016, **88**, 8289–8293.

4 Z. Liu, W. Wang, R. Xie, X.-J. Ju and L.-Y. Chu, *Chem. Soc. Rev.*, 2016, **45**, 460–475.
5 R. Zhang, T. Zhou, H. Peng, M. Li, X. Zhu and Y. Yao, *J. Membr. Sci.*, 2019, **580**, 117–124.
6 C. M. Khor, X. Zhu, M. S. Messina, S. Poon, X. Y. Lew, H. D. Maynard and D. Jassby, *ACS Mater. Lett.*, 2019, **1**, 647–654.
7 S. Baek, S.-R. Kwon, K. Fu and P. W. Bohn, *ACS Appl. Mater. Interfaces*, 2020, **12**, 55116–55124.
8 Q. Yuan, R. Venkatasubramanian, S. Hein and R. D. K. Misra, *Acta Biomater.*, 2008, **4**, 1024–1037.
9 K.-N. Yang, C.-Q. Zhang, W. Wang, P. C. Wang, J.-P. Zhou and X.-J. Liang, *Cancer Biol. Med.*, 2014, **11**, 34–43.
10 I. R. Fernando, D. P. Ferris, M. Frasconi, D. Malin, E. Strekalova, M. D. Yilmaz, M. W. Ambrogio, M. M. Algaradah, M. P. Hong, X. Chen, M. S. Nassar, Y. Y. Botros, V. L. Cryns and J. F. Stoddart, *Nanoscale*, 2015, **7**, 7178–7183.
11 Y.-S. Huang, J.-K. Chen, S.-W. Kuo, Y.-A. Hsieh, S. Yamamoto, J. Nakanishi and C.-F. Huang, *Polymers*, 2019, **11**, 1079.
12 A. Tufani and G. Ozaydin Ince, *J. Membr. Sci.*, 2017, **537**, 255–262.
13 S. Kim, Y. L. Traore, E. A. Ho, M. Shafiq, S. H. Kim and S. Liu, *Acta Biomater.*, 2018, **82**, 12–23.
14 X. Guo and M. Ballauff, *Phys. Rev. E: Stat., Nonlinear, Soft Matter Phys.*, 2001, **64**, 051406.
15 N. Su, H. Li, Y. Huang and X. Zhang, *J. Nanomater.*, 2015, **2015**, 956819.
16 X. Guo and M. Ballauff, *Langmuir*, 2000, **16**, 8719–8726.
17 D. Li, Q. He, Y. Cui and J. Li, *Chem. Mater.*, 2007, **19**, 412–417.
18 L. Zhou, J. Yuan, W. Yuan, X. Sui, S. Wu, Z. Li and D. Shen, *J. Magn. Magn. Mater.*, 2009, **321**, 2799–2804.
19 J. Xie, K. Nakai, S. Ohno, H.-J. Butt, K. Koynov and S.-I. Yusa, *Macromolecules*, 2015, **48**, 7237–7244.
20 S. Sekar, J. Giermanska, H. Saadaoui and J.-P. Chapel, *Colloids Surf., A*, 2016, **500**, 98–104.
21 J. C. Conrad and M. L. Robertson, *Curr. Opin. Solid State Mater. Sci.*, 2019, **23**, 1–12.
22 O. V. Borisov and E. B. Zhulina, *Eur. Phys. J. B*, 1998, **4**, 205–217.
23 R. Hariharan, C. Biver, J. Mays and W. B. Russel, *Macromolecules*, 1998, **31**, 7506–7513.
24 A. S. Lee, V. Bütün, M. Vamvakaki, S. P. Armes, J. A. Pople and A. P. Gast, *Macromolecules*, 2002, **35**, 8540–8551.
25 J. K. Riley, K. Matyjaszewski and R. D. Tilton, *Langmuir*, 2014, **30**, 4056–4065.
26 D. Iqbal, J. Yan, K. Matyjaszewski and R. D. Tilton, *Colloid Polym. Sci.*, 2020, **298**, 35–49.
27 G. Li, J. Xu, S. Zhao, Y. Zhu, L. Li and X. Guo, *Z. Phys. Chem.*, 2012, **226**, 613–623.
28 O. Ueberschär, C. Wagner, T. Stangner, C. Gutsche and F. Kremer, *Polymer*, 2011, **52**, 1829–1836.
29 R. D. Wesley, T. Cosgrove, L. Thompson, S. P. Armes, N. C. Billingham and F. L. Baines, *Langmuir*, 2000, **16**, 4467–4469.
30 P. Pincus, *Macromolecules*, 1991, **24**, 2912–2919.
31 E. B. Zhulina and O. V. Borisov, *Macromolecules*, 1996, **29**, 2618–2626.
32 Z. Ye, L. Li, F. Zhao, Y. Tian, Y. Wang, Q. Yang, L. Dai and X. Guo, *J. Polym. Sci., Part B: Polym. Phys.*, 2019, **57**, 738–747.
33 C. Zhang, T. Carlson, S. Yang and P. Akcora, *Adv. Mater. Interfaces*, 2018, **5**, 1701318.
34 T.-H. Li, V. Yadav, J. C. Conrad and M. L. Robertson, *ACS Macro Lett.*, 2021, **10**, 518–524.
35 V. Yadav, A. V. Harkin, M. L. Robertson and J. C. Conrad, *Soft Matter*, 2016, **12**, 3589–3599.
36 V. Yadav, Y. A. Jaimes-Lizcano, N. K. Dewangan, N. Park, T.-H. Li, M. L. Robertson and J. C. Conrad, *ACS Appl. Mater. Interfaces*, 2017, **9**, 44900–44910.
37 B. J. Frisken, *Appl. Opt.*, 2001, **40**, 4087–4091.
38 F. E. Critchfield, J. A. Gibson and J. L. Hall, *J. Am. Chem. Soc.*, 1953, **75**, 6044–6045.
39 D. H. S. Ramkumar and A. P. Kudchadker, *J. Chem. Eng. Data*, 1989, **34**, 463–465.
40 O. Colombani, E. Lejeune, C. Charbonneau, C. Chassenieux and T. Nicolai, *J. Phys. Chem. B*, 2012, **116**, 7560–7565.
41 F. A. Plamper, H. Becker, M. Lanzendörfer, M. Patel, A. Wittemann, M. Ballauff and A. H. E. Müller, *Macromol. Chem. Phys.*, 2005, **206**, 1813–1825.
42 A. Laguecir, S. Ulrich, J. Labille, N. Fatin-Rouge, S. Stoll and J. Buffle, *Eur. Polym. J.*, 2006, **42**, 1135–1144.
43 J. Fresnais, M. Yan, J. Courtois, T. Bostelmann, A. Bée and J. F. Berret, *J. Colloid Interface Sci.*, 2013, **395**, 24–30.
44 F. Uhlík, P. Košovan, Z. Limpouchová, K. Procházka, O. V. Borisov and F. A. M. Leermakers, *Macromolecules*, 2014, **47**, 4004–4016.
45 C. Dolce and G. Mériguet, *Colloid Polym. Sci.*, 2017, **295**, 279–287.
46 S. Liufu, H. Xiao and Y. Li, *J. Colloid Interface Sci.*, 2005, **281**, 155–163.
47 R. Hariharan, C. Biver and W. B. Russel, *Macromolecules*, 1998, **31**, 7514–7518.
48 P. M. Dodd and A. Jayaraman, *J. Polym. Sci., Part B: Polym. Phys.*, 2012, **50**, 694–705.
49 R. Whitfield, N. P. Truong, D. Messmer, K. Parkatzidis, M. Rolland and A. Anastasaki, *Chem. Sci.*, 2019, **10**, 8724–8734.
50 J. Choi, C. M. Hui, M. Schmitt, J. Pietrasik, S. Margel, K. Matyjazsewski and M. R. Bockstaller, *Langmuir*, 2013, **29**, 6452–6459.

